

# Conductivity of graphene: How to distinguish between samples with short and long range scatterers

Maxim Trushin and John Schliemann

*Institute for Theoretical Physics, University of Regensburg, D-93040 Regensburg, Germany*

Applying a quasiclassical equation to carriers in graphene we found a way how to distinguish between samples with the domination of short and long range scatterers from the conductivity measurements. The model proposed explains recent transport experiments with chemically doped as well as suspended graphene.

## INTRODUCTION

To understand the spectacular transport properties of single graphite layers [1, 2] one has to know which kind of scatterers dominates in a given sample. Indeed, theory predicts the electrical conductivity to be strongly dependent on the particular type of the scatterers being present in the system [3]. We demonstrate that the diversity of the conductivity behaviour observed in graphene [4, 5, 6, 7, 8] can be naturally described employing the concentrations of long and short range scatterers as parameters. According to our microscopic model, the conductivity measurements upon potassium doping [4] obviously suggest a strong domination of the long range scattering potential at all possible carrier concentrations, whereas the nitrogen dioxide doping [5] induces charged impurities dominating the scattering mechanisms near the conductivity minimum only. In addition, we shall see that zero chemical doping gives rise to the very sharp minimum conductivity dip observed in Refs. [7, 8]. Our semiclassical approach fully incorporates the chiral nature of electronic states in graphene which is crucial for a correct description of transport properties.

There are three most important regimes to consider: (I) — *Long range scattering potential limit*. The long range potential of charged impurities strongly dominates the scattering processes and governs *both* the carrier mobility and the conductivity minimum, as shown in fig. 1 and observed in Ref. [4]. Here, the width of the minimum conductivity region is rather broad, with a well defined plateau, and the conductivity minimum itself is around the universal value  $4e^2/h$ . Upon further chemical doping the carrier mobility decreases, the conductivity as a function of carrier concentration above its minimum becomes more linear, whereas the residual conductivity defined by the linear fit keeps constant near  $2e^2/h$ . (II) — *Both long and short range scattering potentials are in play*. At somewhat lower charged impurity concentration, the long range scatterers do not play an essential role in the conductivity behaviour far away from the conductivity minimum. Here, the short range scatterers (i. e. nano-sized ripples [9] and other imperfections [10]) govern the carrier mobility which is defined by the linear fit as shown fig. 2 and, thus, turns out to be insensitive to the chemical doping, as observed in Ref. [5].

The minimum conductivity dip is rather sharp, i. e. no plateau is unambiguously visible. The conductivity minimum is still around  $4e^2/h$ , whereas the residual conductivity can acquire a wide range of values depending on the scattering parameters. (III) — *Short range scattering potential limit*. If the concentration of the long range scatterers vanishes then the minimum conductivity dip becomes very sharp as it is shown in fig. 3 and observed in Refs. [7, 8]. Moreover, at zero concentration of long range scatterers the conductivity minimum becomes indistinguishable from its residual value which is not universal and can reach the values up to tens of  $e^2/h$  as observed in Ref. [6]. Thus, in this latter case both the minimum conductivity dip and carrier mobility are governed by the short range scatterers.

To describe these three cases theoretically we choose a quasiclassical Boltzmann approach since it allows us to get transparent analytical formulas for the electrical conductivity in a broad range of parameters. The most of the previous attempts [11, 12, 13, 14, 15] based on the Boltzmann equation discard the chirality of low energy excitations, and we argue that a proper model must necessarily contain *both* peculiar properties of carriers in graphene, namely, the linear spectrum of low energy excitations *and* its chiral nature. The quasiclassical approach looks at the first sight inapplicable to investigate the conductivity near its minimum since it is expected to fail at low Fermi energies  $E_F$  as soon as  $E_F\tau(E_F)$  becomes comparable with  $\hbar$ . Note, however, that the relaxation time  $\tau$  for short range scatterers diverges [3] at  $E_F = 0$  that leads to a constant product  $E_F\tau(E_F)$  larger than  $\hbar$ . Moreover, as we shall see below, for the long range impurity potentials the conductivity approaches its minimum away from the Dirac point which makes the quasiclassical model applicable again.

We start from the Dirac Hamiltonian  $H_0 = \hbar v_0(\sigma_x k_x + \sigma_y k_y)$  describing the low energy excitations in the  $\pi$ -system of graphene around the  $K$  corner of the first Brillouin zone. [Here  $v_0 \approx 10^6 \text{ms}^{-1}$  is the effective “speed of light”,  $\sigma_{x,y}$  are the Pauli matrices describing the pseudo- (or sublattice-) spin, and  $\mathbf{k}$  is the two-component particle momentum.] To simplify the model we adopt the valley and spin degeneracy of the electron states, see Appendix

for details. The eigenstates have the form

$$\Psi_{\mathbf{k}\pm}(x, y) = \frac{1}{\sqrt{2}} e^{ik_x x + ik_y y} \begin{pmatrix} 1 \\ \pm e^{i\theta} \end{pmatrix}, \quad (1)$$

where  $\tan \theta = k_y/k_x$ , and the energy spectrum reads  $E_{k\pm} = \pm \hbar v_0 k$ . The spinors (1) contain momentum-dependent phase factor  $e^{i\theta}$  which entangles the momentum and the sublattice degree of freedom. This chirality of electronic states plays a crucial role in our description.

To consider both short and long range scatterers on the one hand and to avoid having too many fitting parameters on the other, we choose two opposite types of scattering potential, namely,  $U_0(\mathbf{r}) = \lim_{\varrho \rightarrow R} U(\mathbf{r})$  (with  $R$  being the radius of the short range scatterers), and  $U_1(\mathbf{r}) = \lim_{\varrho \rightarrow \infty} U(\mathbf{r})$ , where  $U(\mathbf{r})$  is the generic one given by  $U(\mathbf{r}) = (u_0/r)e^{-r/\varrho}$ . Assuming that the short and long range scatterers have the concentrations  $N_0$  and  $N_1$  respectively, it is easy to derive the corresponding relaxation times [3] given by

$$\tau_0 = \frac{1}{4\pi R^2 n_0 v_0 k} \frac{2R^4 k^4}{1 + 2R^2 k^2 - \sqrt{1 + 4R^2 k^2}}, \quad (2)$$

$$\tau_1 = \frac{k}{4\pi n_1 v_0}, \quad (3)$$

where  $n_{0,1} = \pi N_{0,1} (2u_0/\hbar v_0)^2$  are the renormalised concentrations being only the two fitting parameters. The characteristic size  $R$  of ripples and other imperfections is assumed to be near a few nm.

To incorporate the chiral nature of Dirac fermions into the stationary quasiclassical kinetic equation linear in the homogeneous electric field  $\mathbf{E}$  we have to start from its general form

$$\frac{1}{\hbar} \left( e\mathbf{E} \frac{\partial \hat{f}}{\partial \mathbf{k}} + i \left[ H_0, \hat{f}(\mathbf{k}) \right] \right) = \mathcal{I}[\hat{f}], \quad (4)$$

where  $\hat{f}$  is the density matrix,  $\mathcal{I}[\hat{f}]$  is the collision integral. In eq. (4), the sublattice degree of freedom is assumed to be a quantum number, although the particle momentum  $\mathbf{k}$  is still considered quasiclassically. To deal with such an equation it is natural to rewrite it in the basis of the eigenvectors (1). The distribution function  $f$  represents then a  $2 \times 2$  matrix, and its off-diagonal elements do not drop out thanks to the chiral nature of the eigenstates (1). This important modification of the Boltzmann equation allows us to deal with the essentially quantum effect suggesting that a particle could not only be in one of the states  $\Psi_{\mathbf{k}+}$  or  $\Psi_{\mathbf{k}-}$  but in an arbitrary superposition of them. Alternatively one might think about the off-diagonal elements as a manifestation of the *pseudospin* precession [2] associated with the chirality index  $\kappa$ .

To solve the kinetic equation with respect to  $f$  we assume the linear response regime (small  $\mathbf{E}$ ). All technical details concerning the kinetic equation, its solution,

and derivation of conductivity expressions are given in the Appendix section. To write down the final zero-temperature conductivity formula it is convenient to introduce the following parameters:  $\gamma_0 = \pi R^2 n_0$  and  $\gamma_n = \pi R^2 n$ , where  $n = k_F^2/\pi$  is the carrier concentration with  $k_F = E_F/\hbar v_0$  being the Fermi wave vector. Then, the conductivity reads

$$\sigma = \frac{e^2}{h} \left\{ \frac{n\gamma_n}{n_0(1 + 2\gamma_n - \sqrt{1 + 4\gamma_n}) + 2n_1\gamma_n} + \frac{2n_1}{n} + 4\gamma_0 \left[ \frac{3}{8} \frac{1}{\gamma_n^2} + \frac{1}{2\gamma_n} + \sqrt{1 + 4\gamma_n} \left( \frac{1}{4\gamma_n} - \frac{3}{8} \frac{1}{\gamma_n^2} \right) - \ln \left( \frac{1}{2\sqrt{\gamma_n}} + \sqrt{1 + \frac{1}{4\gamma_n}} \right) \right] \right\} + \sigma_{\text{res}}^{\text{long}}. \quad (5)$$

The sharp peak at  $n = 0$  in eq. (5) due to the term  $\propto 2n_1/n$  should be seen as an artifact since our quasiclassical approach certainly fails in this limit. According to the experimental data there is normally a plateau instead of that peak. We define the residual conductivity  $\sigma_{\text{res}}^{\text{long}}$  from the linear fit for the conductivity measurements in the limit of long range scatterers domination, as explained in Ref. [4]. As follows from the measurements [4],  $\sigma_{\text{res}}^{\text{long}}$  turns out to be a constant nearly equal to  $2e^2/h$ . The residual conductivity  $\sigma_{\text{res}}^{\text{long}}$  is the only parameter that could not be derived within our quasiclassical approach because of the obvious restriction discussed before. But it contributes to  $\sigma(n)$  in a very simple way:  $\sigma_{\text{res}}^{\text{long}} = 2e^2/h$  just shifts all the  $\sigma(n)$  curves into the region of higher conductivities and does not have an influence on the quasiclassical physics above  $\sigma_{\text{res}}^{\text{long}}$ . Note, however, that the residual conductivity is not a constant as soon as the long range scatterers do not dominate any more. Such residual conductivity  $\sigma_{\text{res}}^{\text{short}} > \sigma_{\text{res}}^{\text{long}}$  can be derived within our approach since it remains valid for short range scatterers even at zero carrier concentration. Note, that eq. (5) is true for arbitrary values of  $n_{0,1}$  and  $R$ , thus, we can utilise this formula to distinguish the transport regimes with the domination of short or long range scatterers. To proceed we set  $R = 1$  nm, thus  $\gamma_n \ll 1$  for all reasonable carrier concentrations, and, as consequence,  $\gamma_0 \ll 1$  as well.

## (I) — LONG RANGE SCATTERING POTENTIAL LIMIT

Long range scatterers dominate if  $n_1 \geq n_0$ . Here, eq. (5) can be expanded in terms of  $\gamma_n$  and  $\gamma_n n_0/n_1$  resulting in the following expression

$$\sigma^{\text{long}} = \frac{e^2}{h} \left[ \frac{n}{2n_1} + \frac{2n_1}{n} + \gamma_0 \left( 5 + 2 \ln \gamma_n - \frac{n^2}{2n_1^2} \right) \right] + \sigma_{\text{res}}^{\text{long}}, \quad (6)$$

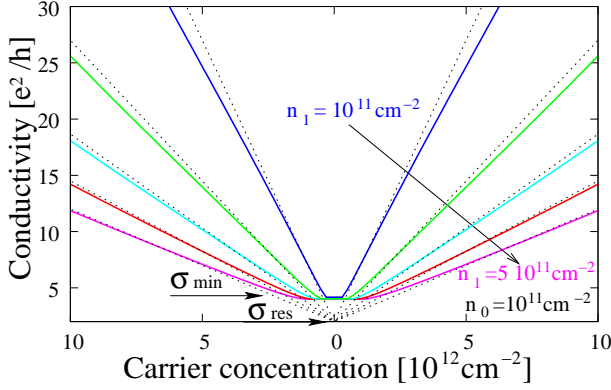


FIG. 1: Conductivity vs. carrier concentration: Domination of the long range scatterers with the renormalised concentration  $n_1$  [defined below eqs. (2–3)] which increases for each curve from 0.1 (upper curve) to 0.5 [ $\times 10^{12} \text{ cm}^{-2}$ ] with  $0.1 \cdot 10^{12} \text{ cm}^{-2}$  step. The renormalised concentration of the short range scatterers  $n_0$  [defined below eqs. (2–3)] keeps constant at  $0.1 \cdot 10^{12} \text{ cm}^{-2}$ . Dotted lines are the linear approximations given by  $\sigma^{\text{long}} = e\mu^{\text{long}}n + \sigma_{\text{res}}^{\text{long}}$  where  $\mu^{\text{long}} = e/(2\hbar n_1)$  (with  $\hbar = 2\pi\hbar$  being the Planck constant) is the carrier mobility obviously governed by the long range scatterers. The conductivity minimum  $\sigma_{\text{min}}$  is close to  $4e^2/h$  whereas the residual conductivity  $\sigma_{\text{res}}$  is equal to  $2e^2/h$  and turns out to be independent of  $n_1$ . The sharp peak at  $n = 0$  due to the term  $\propto 2n_1/n$  in eq. (6) has been removed as an artifact. This transport regime corresponds to the graphene samples strongly doped by potassium [4].

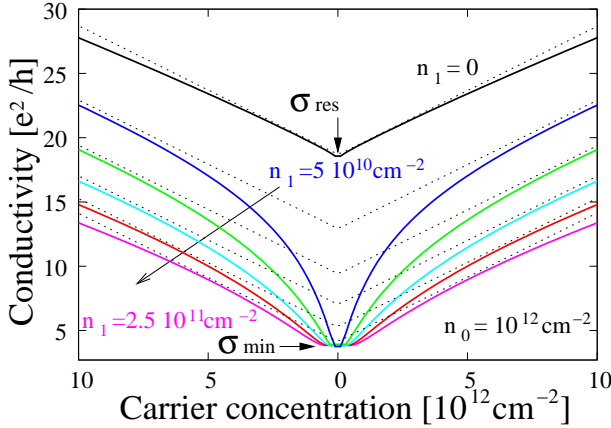


FIG. 2: Conductivity vs. carrier concentration: Both long and short range scattering potentials contribute essentially. The renormalised concentration of short range scatterers  $n_0$  is assumed to be a constant  $10^{12} \text{ cm}^{-2}$ , whereas the concentration of long range scatterers  $n_1$  increases for each curve from zero (upper curve) to  $0.25 \cdot 10^{12} \text{ cm}^{-2}$  with  $0.05 \cdot 10^{12} \text{ cm}^{-2}$  step. Dotted lines are the linear approximations given by  $\sigma^{\text{short}} = e\mu^{\text{short}}n + \sigma_{\text{res}}^{\text{short}}$  with the carrier mobility  $\mu^{\text{short}} = e/(\hbar n_0)$  governed by the short range scatterers and  $\sigma_{\text{res}}^{\text{short}}$  defined by fit. Though the conductivity minimum is still near  $4e^2/h$  and does not depend strongly on the impurity concentration  $n_1$ , the residual conductivity depends on both concentrations for short and long range scatterers, see the main text. This transport regime corresponds to the graphene samples doped by nitrogen dioxide [5].

$$\sigma_{n_0=0}^{\text{long}} = \frac{e^2}{h} \left( \frac{n}{2n_1} + \frac{2n_1}{n} \right) + \sigma_{\text{res}}^{\text{long}}, \quad n_0 = 0. \quad (7)$$

The function  $\sigma^{\text{long}}(n)$  has a minimum near  $n_{\text{min}} = 2n_1$ ,  $n_1 \neq 0$ . At this concentration the term proportional to  $\gamma_0$  is much smaller than the leading one, and the conductivity reaches its minimum close to  $\sigma_{\text{min}}^{\text{long}} = \sigma_{\text{res}}^{\text{long}} + 2e^2/h$  as it is seen in fig. 1. Since  $\sigma_{\text{res}}^{\text{long}} = 2e^2/h$  the conductivity minimum indeed acquires the typical value  $4e^2/h$  in quite perfect samples (i. e. without ripples, neutral impurities etc.) when  $\gamma_0 \rightarrow 0$ . The corrections of the order of  $o(\gamma_0)$  and  $o(\gamma_0 \ln \gamma_n)$  give all together a small negative contribution to the conductivity minimum. Most importantly, the conductivity minimum does not depend on  $n_1$ , i. e. it should be insensitive to doping, whereas the minimum carrier concentration  $n_{\text{min}} = 2n_1$  increases linearly with chemical doping and in that way gives rise to the width of the minimum conductivity plateau, as observed in [4]. Above  $n = n_{\text{min}}$  (i. e.  $n \gg 2n_1$ ) one can linearise eq. (6) and obtain  $\sigma^{\text{long}} = e\mu^{\text{long}}n + \sigma_{\text{res}}^{\text{long}}$  with  $\mu^{\text{long}} = e/(2\hbar n_1)$  being the carrier mobility. The deviations from linear dependency  $\sigma^{\text{long}}(n)$  are described by the term  $\propto -n^2/2n_1^2$  in eq. (6) and can be seen in fig. 1 as well. All these peculiar features indicate the domination of long range scatterers that was observed in [4].

## (II) — BOTH LONG AND SHORT RANGE SCATTERING POTENTIALS ARE IN PLAY

At lower charged impurity concentrations the minimum conductivity dip becomes sharper, the plateau vanishes, and the carrier mobility is governed by the short range scatterers, see fig. 2. For large enough carrier concentrations so that  $n_0\gamma_n \gg n_1$  the conductivity can be written as

$$\sigma^{\text{short}} = \frac{e^2}{h} \left[ \frac{1}{2\gamma_0} \left( 1 - \frac{n_1}{n_0} \frac{1}{\gamma_n} \right) + \frac{n}{n_0} \right] + \sigma_{\text{res}}^{\text{long}}. \quad (8)$$

We emphasise that eq. (8) is just an estimate for the conductivity far away from its minimum, i. e. for the carrier concentrations  $n \gg n_1/\gamma_0$ . Eq. (8) allows us to define the carrier mobility as  $\mu^{\text{short}} = e/(\hbar n_0)$  and residual conductivity  $\sigma_{\text{res}}^{\text{short}} = \frac{e^2}{h} \frac{1}{2\gamma_0} \left( 1 - \frac{n_1}{n_0} \frac{1}{\gamma_N} \right) + \sigma_{\text{res}}^{\text{long}}$  with  $\gamma_N$  being  $\gamma_n$  taken at  $n = N$  large enough to satisfy  $N \gg n_1/\gamma_0$ . Though the estimation for  $\sigma_{\text{res}}^{\text{short}}$  is very rough [since eq. (8) is an estimate as well], it shows that the residual conductivity is not a constant anymore as long as the short range scatterers dominate. Thus, the residual conductivity depends on both short and long range scatterers, whereas the conductivity minimum is governed by the long range scatterers alone and remains near the typical value  $4e^2/h$ , as one can observe in fig. 2. The latter is due to the fact that  $\tau_1 \ll \tau_0$  at vanishing carrier density even if  $n_0 \gg n_1$ . On the other hand, the

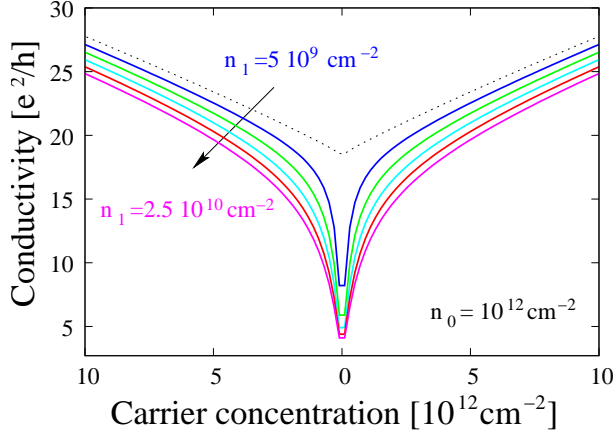


FIG. 3: Conductivity vs. carrier concentration: Domination of the short range scatterers with the renormalised concentration  $n_0 = 10^{12} \text{ cm}^{-2}$ . The renormalised concentration of long range scatterers  $n_1$  increases for each curve from  $5 \cdot 10^9 \text{ cm}^{-2}$  (upper curve) to  $2.5 \cdot 10^{10} \text{ cm}^{-2}$  with  $5 \cdot 10^9 \text{ cm}^{-2}$  step. The dotted line corresponds to the case  $n_1 = 0$ . The conductivity dip is very sharp and does not contain a plateau. According to the very recent report [7], the conductivity of suspended graphene after annealing indeed demonstrates very sharp dip at zero gate voltages. Comparison of the conductivity measurements for suspended and non-suspended graphene [8] is also consistent with our predictions.

carrier mobility  $\mu^{\text{short}}$  depends on  $n_0$  and, thus, is unaffected by the chemical doping. Such behaviour indicates the short range scatterers domination in the conductivity measurements upon nitrogen dioxide doping [5].

### (III) — SHORT RANGE SCATTERING POTENTIAL LIMIT

It is instructive to consider the special case  $n_1 = 0$  in detail. Here the term  $\propto 2n_1/n$  does not dominate over the logarithmic one  $\propto \ln \gamma_n$  at  $n \rightarrow 0$ , and, therefore, the latter must be retained. The conductivity then reads

$$\sigma_{n_1=0}^{\text{short}} = \frac{e^2}{h} \left( \frac{1}{2\gamma_0} + \frac{n}{n_0} + 2\gamma_0 \ln \gamma_n \right) + \sigma_{\text{res}}^{\text{long}}. \quad (9)$$

Interestingly, the conductivity minimum is uncertain, but since  $R$  is small ( $\gamma_{0,n} \ll 1$ ) the conductivity at  $n \rightarrow 0$  is indeed indistinguishable from its residual value  $\sigma_{\text{res}}^{\text{short}}(n_1 = 0) = \frac{e^2}{h} \frac{1}{2\gamma_0} + \sigma_{\text{res}}^{\text{long}}$ . This case is depicted in fig. 3 and corresponds to the chemically undoped [6] and suspended [7, 8] graphene samples where the conductivity demonstrates rather sharp dip with nonuniversal minimum value strongly dependent on scattering parameters. It is noteworthy that similar logarithmic corrections to the conductivity minimum have been found in presence of electron-electron interactions [16, 17] and scattering on vacancies, cracks, or boundaries [14].

Given the above theoretical results, let us now analyse recent experiments on graphene samples upon chemical doping [4, 5]. We first discuss the case of potassium doping [4]. Here, the width of the minimum conductivity region broadens (i. e.  $n_{\text{min}}$  increases) whereas both the minimum conductivity and mobility decrease, at least initially. At certain stage, however, the conductivity minimum becomes insensitive to further doping. These features are clearly understood within our model. Initially, the sample is very weakly doped, and the minimum conductivity is governed by the short range scatterers rather than charged impurities in accordance with eq. (9). At larger potassium concentrations the long range scatterers start to dominate, the minimum concentration  $n_{\text{min}} \propto n_1$  increases whereas the conductivity minimum keeps constant despite further decreasing the mobility. This limit corresponds to eq. (7). In Ref. [5], graphene is doped by nitrogen dioxide. Here, the width of the conductivity minimum region broadens similar to the previous case but it remains much more narrow than upon potassium doping. Moreover, the carrier mobility and conductivity minimum are both insensitive to doping. According to eq. (8) such data suggest strong domination of the short range scatterers, at least at higher carrier concentrations  $n \gg n_1/\gamma_0$ . The reason of such a strong suppression of induced charges might be the strong screening of Coulomb interactions in the samples examined. Such precise description of charged impurities is certainly beyond the scope of this report, where  $U_1$  is not screened at all. We can predict, however, that the minimum conductivity phenomenon takes place even in free hanging graphene sheets, without any influence of the silicon dioxide substrate considered in [15].

Moreover, our model offers a solution to the urgent minimum conductivity problem. Previous measurements appear to be contradictory in so far as quite a representative group of graphene samples [1] exhibits the conductivity minimum clustering around  $4e^2/h$ , whereas many other samples [6] demonstrate very wide range of the minimum conductivity values, away from  $4e^2/h$ . Now it is clear that the universal conductivity minimum in the samples from [1] is due to the long range scatterers (e. g. charged impurities) with a little influence of ripples and other short range imperfections. This results in the conductivity dip broaden enough to resolve its bottom at  $\sigma \sim 4e^2/h$ . (The carrier mobility, however, is not necessarily governed by charged impurities.) In contrast, the conductivity minimum far away from  $4e^2/h$  betrays the lack of the charged impurities in a given sample that makes the conductivity dip sharper and its bottom difficult to resolve, as it is seen from eq. (9). Thus, the minimum conductivity becomes indistinguishable from its residual value which, in general, is sensitive to the concentrations of both long and short range scatterers. It is therefore not surprising that the conductivity minimum changes from sample to sample in this case. In

that way our model is able to explain the wide diversity of the minimum conductivity values measured in single layer graphene.

As an important further conclusion we would like to emphasise that it is the chiral nature of low energy excitations, rather than its linear spectrum, that is responsible for the minimum conductivity phenomenon in graphene. It is especially obvious for quite perfect graphene samples where long range scatterers (i. e. charged impurities) dominate the scattering processes: The conductivity would be given just by the first term in eq. (7), and the conductivity minimum would certainly vanish as long as the chiral nature were discarded. Such a conclusion is consistent with the theoretical investigation of ballistic graphene [18] and strongly supported by the very experimental fact that bilayer graphene, despite obviously non-linear dispersion law, also exhibits a minimum conductivity of the same order as single layer samples [1]. The conductivity measurements for chemically doped bilayer samples are not accessible yet, they would certainly be an *experimentum crucis* on which the mechanism is responsible for the conductivity minimum in graphene.

## APPENDIX — SOLUTION OF THE KINETIC EQUATION

The distribution function  $f(\mathbf{k})$  for carriers in presence of the electric field  $\mathbf{E}$  can be written as the sum of an equilibrium contribution  $f^0(E_{k\kappa})$  (which is just the Fermi function) and a nonequilibrium part  $f^1(\mathbf{k})$  which represents a  $2 \times 2$  matrix. To find  $f^1(\mathbf{k})$  one has to solve eq. (4) written in the helicity basis (1). To do that one has to bear in mind that the spinors are  $\mathbf{k}$ -dependent (via the phase  $i\theta$ ), thus, the kinetic equation differs from its standard analogue and reads

$$\begin{aligned} I[f] = & \frac{i}{\hbar} \begin{pmatrix} 0 & f_{12}(E_{k+} - E_{k-}) \\ f_{21}(E_{k-} - E_{k+}) & 0 \end{pmatrix} \\ & + e\mathbf{E} \begin{pmatrix} -\mathbf{v}_{11} \left[ -\frac{\partial f^0(E_{k+})}{\partial E_{k+}} \right] & \frac{\mathbf{v}_{12}}{2E_{k+}} \left( f_{E_{k-}}^0 - f_{E_{k+}}^0 \right) \\ \frac{\mathbf{v}_{21}}{2E_{k-}} \left( f_{E_{k+}}^0 - f_{E_{k-}}^0 \right) & -\mathbf{v}_{22} \left[ -\frac{\partial f^0(E_{k-})}{\partial E_{k-}} \right] \end{pmatrix} \end{aligned} \quad (10)$$

with  $\mathbf{v}_{ij}$  being the velocity matrix elements given by

$$\frac{\mathbf{v}}{v_0} = \mathbf{e}_x \begin{pmatrix} \cos \theta & -i \sin \theta \\ i \sin \theta & -\cos \theta \end{pmatrix} + \mathbf{e}_y \begin{pmatrix} \sin \theta & i \cos \theta \\ -i \cos \theta & -\sin \theta \end{pmatrix}. \quad (11)$$

One might ask why spin and valley degrees of freedom are discarded in eq. (10). The reason is that the total Hamiltonian  $H$  (which includes, in addition to the sublattice index  $\kappa$ , the spin  $s$  and valley  $\nu$  indices) does not contain the crossing (off-diagonal) terms  $H^{ss'}$  and  $H^{\nu\nu'}$ , and, therefore spin and valley coherence does not manifest itself in the conductivity. In contrast, the sublattice

degree of freedom couples electron and hole states via the off-diagonal terms  $H_0^{\kappa\kappa'}$  in the Hamiltonian  $H_0$  that leads to the non-diagonal velocity operator and electron-hole coherent contributions in the conductivity.

To find the collision integral in eq. (10) we start from the commutator  $-\frac{i}{\hbar}[U, \hat{f}]$ , where the density matrix is substituted by the following expression describing its time evolution after each scattering event

$$\hat{f} \rightarrow \hat{f}(t=0) + \frac{i}{\hbar} \int_0^\infty dt e^{-\frac{i}{\hbar} H_0 t} [\hat{f}(t=0), U] e^{\frac{i}{\hbar} H_0 t}. \quad (12)$$

The integrals over  $t$  can be taken introducing a small parameter in the time dependent exponent

$$\int_0^\infty dt e^{\frac{i}{\hbar}(E_{\mathbf{k}'\kappa'} - E_{\mathbf{k}\kappa})t} = P \frac{i\hbar}{E_{\mathbf{k}'\kappa'} - E_{\mathbf{k}\kappa}} + \pi \hbar \delta(E_{\mathbf{k}'\kappa'} - E_{\mathbf{k}\kappa}), \quad (13)$$

where  $P$  denotes the principle value. Then the collision integral reads

$$\begin{aligned} I[f]_{\kappa\kappa'} = & \int \frac{d^2\mathbf{k}'}{(2\pi)^2} \sum_{\kappa_1, \kappa'_1} \{ [\delta(E_{k'\kappa_1} - E_{k\kappa}) \\ & + \delta(E_{k'\kappa'_1} - E_{k\kappa'})] K_{\kappa_1\kappa'_1}^{\kappa\kappa'} f_{\kappa_1\kappa'_1}(k') - \delta(E_{k\kappa_1} - E_{k'\kappa'_1}) \\ & \times [K_{\kappa'_1\kappa_1}^{\kappa\kappa'} f_{\kappa_1\kappa'}(k) + f_{\kappa\kappa_1}(k) K_{\kappa'_1\kappa'_1}^{\kappa\kappa'}] \}, \end{aligned} \quad (14)$$

with  $K_{\kappa_1\kappa'_1}^{\kappa\kappa'}$  being

$$K_{\kappa_1\kappa'_1}^{\kappa\kappa'} = \frac{\pi}{\hbar} \sum_{i=0,1} \langle \Psi_{\kappa k} | U_i | \Psi_{\kappa_1 k'} \rangle \langle \Psi_{\kappa' k} | U_i | \Psi_{\kappa'_1 k'} \rangle^*.$$

This form of the collision integral describes elastic scattering of chiral particles within Born approximation and is routinely applied to kinetics of chiral electrons with spin-orbit interactions, see e.g. [19, 20]. It is important that the intrinsically inelastic terms [i. e. the principle value in eq. (13)] are discarded in the final expression for  $I[f]$ . These terms describe creation of electron-hole pairs and have been dubbed in [21] as *zitterbewegung* contributions. The latter does not change results qualitatively but essentially complicates the analytics as one can see comparing Refs. [21] and [22]. To reach a compromise between transparency and completeness of our model we deal only with the leading (i. e.  $\delta$ -functional) terms in the collision integral.

The solution of eq. (10) can be written down as  $f(\mathbf{k}) =$

$f^0(E_{k\kappa}) + f^1(\mathbf{k})$ , where

$$f_{11}^1 = q\mathbf{E}\mathbf{v}_{11}\tau(k) \left\{ \left(1 + \frac{1}{2\alpha}\right) \left[-\frac{\partial f^0(E_{k+})}{\partial E_{k+}}\right] + \frac{1}{2\alpha} \left[-\frac{\partial f^0(E_{k-})}{\partial E_{k-}}\right] + \frac{1}{2\alpha E_{k+}} (f_{E_{k+}}^0 - f_{E_{k-}}^0) \right\} \quad (15)$$

$$f_{12}^1 = \frac{q\mathbf{E}\mathbf{v}_{12}\tau(k) \left(\frac{1}{2} + \frac{1}{2\alpha}\right)}{1 + 2iE_{k+}\tau(k)/\hbar} \left\{ \frac{1}{E_{k+}} (f_{E_{k+}}^0 - f_{E_{k-}}^0) + \left[-\frac{\partial f^0(E_{k+})}{\partial E_{k+}} - \frac{\partial f^0(E_{k-})}{\partial E_{k-}}\right] \right\}, \quad (16)$$

and  $f_{22}^1, f_{21}^1$  can be obtained from eqs. (15–16) just exchanging the indices belong to  $E_k$  and  $\mathbf{v}$  accordingly. Here,  $\tau^{-1} = \tau_0^{-1} + \tau_1^{-1}$  is the total momentum relaxation time, and  $\alpha(k) = 4E_{k+}^2\tau^2/\hbar^2$  is the electron-hole incoherence parameter. The off-diagonal elements  $f_{12}^1$  and  $f_{21}^1$  do not contribute to the current if and only if they become real at  $\alpha \gg 1$ .

The electrical current  $\mathbf{j} = e \int \frac{d^2k}{(\pi)^2} \text{Tr} [\mathbf{v}(k)f^1(\mathbf{k})]$  is easy to derive at low temperatures ( $T \ll E_F$ ), and the conductivity can be written as a sum  $\sigma = \mathbf{j}/\mathbf{E} + \sigma_{\text{res}}^{\text{long}}$  with a constant  $\sigma_{\text{res}}^{\text{long}}$  being the residual conductivity in the limit of the long range scatterers domination defined by the linear fit from the experimental data [4]. The formula ( ) follows directly from eqs. (15–16) and is exact in this sense. It is only essential to integrate over  $\mathbf{k}$  before the subsequent approximations relying on a small  $R$ ; we would obtain the logarithmic divergence in the conductivity integral otherwise [21, 22].

This work was financially supported by SFB 689. We thank Mikhail Katsnelson and Tobias Stauber for stimulating discussions.

- [2] Geim A. K. MacDonald A. H. *Physics Today*60200735.
- [3] Castro Neto A. H., Guinea F., Peres N. M. R., Novoselov K. S., and Geim A. K. *The electronic properties of graphene* arXiv:0709.1163.
- [4] Chen J. H., Jang C., Fuhrer M. S., Williams E. D., and Ishigami M. *Charged Impurity Scattering in Graphene* arXiv:0708.2408.
- [5] Schedin F., Geim A. K., Morozov S. V., Hill E. W., Blake P., Katsnelson M. I., Novoselov K. S. *Nat. Mat.*62007652.
- [6] Tan Y.-W., Zhang Y., Bolotin K., Zhao Y., Adam S., Hwang E.H., Das Sarma S., Stormer H. L., Kim. P. *Phys. Rev. Lett.*992007246803.
- [7] Bolotin K. I., Sikes K. J., Jiang Z., Fudenberg G., Hone J., Kim P., Stormer H. L. *Ultrahigh electron mobility in suspended graphene:* arXiv:0802.2389.
- [8] Du X., Li G., Barker A., Andrei E. Y. *Suspended graphene: a bridge to the Dirac point:* arXiv:0802.2933.
- [9] Meyer J. C., Geim A. K., Katsnelson M. I., Novoselov K. S., Booth T. J., Roth. S. *Nature*446200760.
- [10] Katsnelson M. I. Geim, A. K. *Philos. Trans. R. Soc.* A3662008195.
- [11] Nomura K. MacDonald A. H. *Phys. Rev. Lett.*962006256602.
- [12] Ando T. *J. Phys. Soc. Jpn.*75200674716.
- [13] Hwang E. H., Adam S., Das Sarma S. *Phys. Rev. Lett.*982007186806.
- [14] Stauber T., Peres N. M. R., Guinea F. *Phys. Rev. B*762007205423.
- [15] Adam S., Hwang E. H., Galitski V. M., Das Sarma S. *Proc. Natl. Acad. Sci. USA*104200718392.
- [16] Mishchenko E. G. *Phys. Rev. Lett.*982007216801.
- [17] Herbut I. F., Jurić V., Vafek O. *Phys. Rev. Lett.*1002008046403.
- [18] Katsnelson M. I. *Eur. Phys. J. B*512006157.
- [19] D'yakonov M. I., Khaetskii A. V. *JETP*5919841072.
- [20] Khaetskii A. *Phys. Rev. Lett.*96200656602.
- [21] Auslender M., Katsnelson M. I. *Phys. Rev. B*762007235425.
- [22] Trushin M., Schliemann J. *Phys. Rev. Lett.*992007216602.

---

[1] Geim A. K. Novoselov K. S. *Nat. Mat.*62007183.